Edyta Podstawka[1,3]
Piotr J. Mak[1,2]
James R. Kincaid[1]
Leonard M. Proniewicz[2,3]
[1] *Department of Chemistry, Marquette University, Milwaukee, WI 53201-1881 USA*

[2] *Faculty of Chemistry, Jagiellonian University, 3 Ingardena Str., 30-060 Krakow, Poland*

[3] *Regional Laboratory of Physicochemical Analysis and Structural Research, Jagiellonian University, 3 Ingardena Str., 30-060 Krakow, Poland*

Low Frequency Resonance Raman Spectra of Isolated α and β Subunits of Hemoglobin and Their Deuterated Analogues

Received 12 February 2006; revised 26 June 2006; accepted 1 July 2006
Published online 14 July 2006 in Wiley InterScience (www.interscience.wiley.com). DOI 10.1002/bip.20573

Abstract: *In an attempt to gain further insight into the nature of the low frequency vibrational modes of hemoglobin and its isolated subunits, a comprehensive study of several different isotopically labeled analogues has been undertaken and is reported herein. Specifically, the resonance Raman spectra, between 200 and 500 cm^{-1}, are reported for the deoxy and ligated (CO and O_2) forms of the isolated* α *and* β *subunits containing the natural abundance or various deuterated analogues of protoheme. The deuterated protoheme analogues studied include the 1,3,5,8-C^2H_3-protoheme (*d*12- protoheme), the 1,3-C^2H_3-protoheme (1,3-*d*6-protoheme), the 5,8-C^2H_3-protoheme (5,8-*d*6-protoheme), and the meso-C^2H_4-protoheme (*d*4-protoheme). The entire set of acquired spectra has been analyzed using a deconvolution procedure to help correlate the shifted modes with their counterparts in the spectra of the native forms. Interestingly, modes previously associated with so-called vinyl bending modes or propionate deformation modes are shown to be quite sensitive to deuteration of the peripheral methyl groups of the macrocycle, shifting by up to 12–15 cm^{-1}, revealing their complex nature. Of special interest is the fact that shifts observed for the 1,3-*d*6- and 5,8-*d*6-protoheme analogues confirm the fact that certain modes are associated with a given portion of the macrocycle; i.e., only certain modes shift upon deuteration of the 1 and 3 methyl groups, while others shift upon deuteration of the 5 and 8 methyl groups. Compared with the spectra previously reported for the corresponding myoglobin derivatives, the data reported here reveal the appearance*

Correspondence to: J. R. Kincaid; e-mail: james.kincaid@marquette.edu or L. M. Proniewicz; e-mail: proniewi@chemia.uj.edu.pl

Biopolymers, Vol. 83, 455–466 (2006)

of several additional features that imply splitting of modes associated with the propionate groups or that are indicative of greater distortion of the heme prosthetic groups. Biopolymers 83: 455–466, 2006

This article was originally published online as an accepted preprint. The "Published Online" date corresponds to the preprint version. You can request a copy of the preprint by emailing the Biopolymers editorial office at biopolymers@wiley.com

Keywords: *resonance Raman spectroscopy (RR); hemoglobin; selectively deuterated hemes*

INTRODUCTION

The hemoglobin molecule, Hb, is a tetramer that consists of two α and two β chains each containing a protoheme prosthetic group that is bonded to the protein by a single coordinate covalent bond between the heme iron and the imidazole fragment of the proximal histidine.[1] In deoxyHb the heme is domed, with the magnitude of the doming being controlled by steric repulsion between the imidazole and heme macrocycle and effect of the protein tension.[1,2] Binding of exogenous ligands induces changes in the planarity of the heme macrocycle from the domed structure of the deoxy form to more planar configurations.[1,2] In addition to these changes in macrocycle planarity, there are known or potential changes in the disposition of the heme 2- and 4-vinyl groups and the 6- and 7-propionate groups, the latter groups being capable of H-bonding interactions with active site amino acid residues. Such changes in peripheral group orientations between various forms of Mb and Hb have been documented in high resolution crystal structure determinations,[2–6] but may also adopt different functionally significant orientions in various ligation intermediates that cannot be stabilized and studied by X-ray methods. Thus, it is important to develop effective spectroscopic probes of heme protein active site structures that are applicable to both stable forms and these fleeting, functionally significant intermediates.

Resonance Raman (RR) spectroscopy, and its time-resolved extension (TR3) spectroscopy, have proven themselves to be exquisite probes of heme structure for both the stable and intermediate states in heme proteins and enzymes, with comprehensive applications to hemoglobin structural dynamics being pioneered and elegantly refined by Rousseau and Friedman,[7,8] Spiro and coworkers,[9,10] and Kitagawa's group,[11] among others.[12–14] In those studies most attention has been focused on the high frequency, so-called marker, modes that report on heme macrocycle structure and oxidation state.[15,16] The nature of these high frequency structure-sensitive modes has been elucidated by isotopic labeling studies and normal mode calculations.[17–26] Interestingly, in more recent years, it has become increasing apparent that the low frequency RR spectral region (between 200 and 700 cm^{-1}) contains both in-plane and out-of-plane heme deformation modes that are particularly sensitive to peripheral group disposition and their interactions with the active site environment.[27–35] However, to make the most effective use of this spectral sensitivity, it is necessary to gain a deeper understanding of nature of these modes, i.e., to establish which particular molecular fragments participate in a given normal mode. A key step in gaining this information is to test the sensitivity of the given modes to selective isotopic labeling, deuteration being the most accessible form of labeling. To this end we here report the low frequency RR spectra of isolated hemoglobin subunits that have been reconstituted with several selectively deuterated protoheme analogues. Spectra are reported for three physiologically significant forms: the deoxy form, as well as the CO- or O_2-ligated forms. Isotopic substitution of the methyl groups at the 1 and 3 positions (1,3-*d*6-protoheme) (Figure 1)

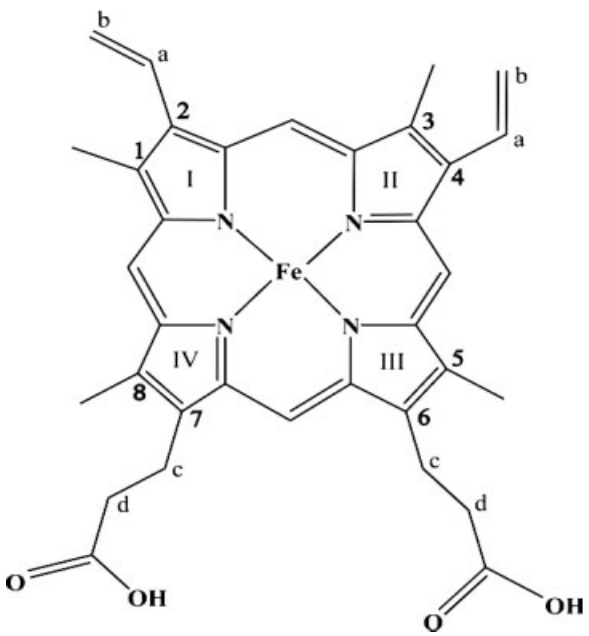

FIGURE 1 Structure and labeling scheme for protoheme IX.

provides information about RR bands associated with I and II pyrrole rings and their peripheral methyl and vinyl groups while deuteration of methyl groups at the 5 and 8 positions (5,8-*d*6-protoheme) can help to establish assignment of Raman modes associated with the III and IV pyrrole rings, which presumably report on movements of the attached propionate groups.[30,31,33] Studies of the methine-deuterated prosthetic group, *d*4-protoheme (Figure 1), are useful to detect low frequency out-of-plane heme macrocycle deformation modes that are expected to be most sensitive to the methine deuteration.[20,36,37] Analysis of the entire set of RR spectra for the isolated subunits and their deuterated analogs in the deoxy, CO, and O_2 forms helps identify which modes are useful for monitoring peripheral group interactions. In addition, the potential utility of such labeled derivatives for documenting subunit heterogeneity within a functioning hemoglobin tetramer is also discussed.

EXPERIMENTAL

Ferriprotoporphyrin IX chloride (Fe^{III}(PPIX)Cl) was purchased from Porphyrin Products, Logan, UT, USA) and used after checking its purity by using thin-layer chromatography (TLC), proton NMR, and electronic absorption spectroscopy.[38–40] All solvents and chemical reagents used in this work were of HPLC or spectroscopic grade, including deuterated methyl sulfoxide (dimethylsulfoxide (DMSO)-d_6), tetrabutylammonium hydroxide (TBAOH), as a 1.0 *M* solution in methanol, anhydrous tetrahydrofuran (THF), and anhydrous hexane. Sodium *p*-(hydroxymercuri)benzoate (PMB) was purchased from Aldrich Chemical Company and used without further purification. Bio-gel P-6DG (Bio-Rad Laboratories, Hercules, CA, USA), CM cellulose (CM-52), and diethylaminoethyl cellulose (DE-53) (Whatman, Fairfield, NJ, USA) were used for protein column chromatography.

Synthesis of Selectively Deuterated Protohemes

Deuterium substitution at the four methine carbons (*d*4-protoheme) and synthesis of 1,3,5,8-$(C^2H_3)_4$-protoheme (*d*12-protoheme) were accomplished according to previously published procedures.[29,30,41,42] Syntheses of 1,3-$(C^2H_3)_2$-protoheme (1,3-*d*6-protoheme) and 5,8-$(C^2H_3)_2$-protoheme (5,8-*d*6-protoheme) were conducted with slight modifications[31] of the procedure used for deuterium substitution of the four methyl groups of protoheme.[30,42] Thin layer chromatography, pyridine hemochromogen electronic absorption spectra, and proton NMR were done to check purity of the final samples of labeled protohemins.[39,43–45] The ^1H NMR spectra (300 Mz) in DMSO-d_6/2 *M* KCN in D_2O (1:6) revealed that the methyl groups in *d*12-protoheme were deuterated to the extent of >95% with little loss (<5%) of the vinyl or propionic protons,[38–40,43] while, in the case of 1,3-*d*6-protoheme, the 1 and 3 methyl groups were deuterated to the extent of 95%, while the 5 and 8 methyl groups remained essentially protonated (90–95%). In the case of the 5,8-*d*6-protoheme sample, the 5 and 8 methyl groups were effectively exchanged (90–95% deuterated), while the 1 and 3 methyl groups showed only 5–10% deuterium substitution.[31] The methine protons in the *d*4-protoheme were deuterated to the extent of 95%.

Protein Preparation

Hemoglobin was isolated from red blood cells according to an established procedure[46] and stored as the CO adduct. ApoHb was prepared by the acid–acetone method.[47] Its reconstitution with different deuterated protohemes to form *d*4-Hb, *d*12-Hb, 1,3-*d*6-Hb, and 5,8-*d*6-Hb was accomplished as described previously.[46,48,49] Reconstituted Hbs were reduced with sodium dithionite under a CO atmosphere and dissociated into their subunits by reaction with PMB[29] followed by column chromatographic separation and purification, as reported in the literature.[49]

Sample Preparation for Raman Measurements

All of the samples were prepared in 0.030 *M* phosphate buffer of pH 7.0 using the following procedures. The carbon monoxide adducts were made by passing CO, with stirring, over a given hemeprotein solution placed in a small round-bottom flask. The dioxygen adducts were obtained by photodissociation (250 W incandescent source) of CO from the sample at 0°C (sample immersed in an ice-water bath) while gently purging the solution with O_2. The resulting oxygenated Hb was transferred to a standard NMR tube and connected to a vacuum line. The samples of deoxyHbs were obtained by evacuation of the oxygenated derivatives on this vacuum line with intermittent flushing with dry, oxygen-free, nitrogen.

Resonance Raman Measurements

Resonance Raman spectra were obtained with a Spex Model 1403 Czerny-Turner double monochromator equipped with a Hamamatsu R928 photomultiplier and Spex monochromator control hardware with SpectraMax/32 software. Excitation at 441.6 (helium: cadmium laser, Liconix model 4240NB) and 413.1 nm (Coherent Model Innova 100-K3 krypton ion laser) were used to measure RR spectra of deoxy forms and ligated species (O_2 and CO) of α and β Hb subunits, respectively. Power at the sample was 10 mW for deoxy and O_2 adducts and 1 mW for CO complexes. The oxy samples were checked for traces of met- form by electronic absorption spectra (Hewlett-Packard Model 8452A diode spectrometer). Before and after measurements, the deoxy samples were checked for traces of dioxy- or metHb (monitoring the ν_4 around 1375 cm^{-1} with the 413.1 nm excitation line). All RR mea-

surements were done at room temperature in spinning NMR tubes (WG-5 M-ECONOMY - O_2 and CO forms, J. Young Valve – deoxy sample, Wilmad, Buena, NJ, USA). To lessen local heating, a small magnetic stirring bar was placed inside the NMR tube and held in a fixed position by an external magnet, while the tube was being spun, i.e., to provide efficient mixing of the protein solution at the point of illumination. Spectral band-pass was set at 4 cm^{-1}. The accuracy of frequency readings was ± 1 cm^{-1}.

Deconvolution Procedure

The spectra presented for the deoxy forms are normalized to the strong ν(Fe-N_{His}) mode near 220 cm^{-1}; it is pointed out that in each of these spectra this mode is broad and at the edge of our measurement window, so the normalization procedure was performed by using one strong band of fixed intensity and frequency (for the native and isotopic analogues), having a 23 cm^{-1} bandwidth, and including a second lower frequency band that was allowed to adjust to fill in the lower frequency edge. The spectra of the native and isotopically labeled analogues of the CO forms were normalized to the ν(Fe-CO) mode at 505 cm^{-1} and those of the oxygenated forms were normalized to the ν(Fe-O_2) modes at 570 cm^{-1}.

Deconvolution of the region from 200 to 450 cm^{-1} for RR spectra of all the α and β deoxy and ligated Hb subunits and their deuterated analogues was conducted using a GRAMS/AI program from Galactic Industries Co. (Salem, NH, USA). Briefly, a 50/50% Lorentzian/Gaussian band shape for all bands was assumed and fixed. The number of bands, their initial frequencies, their bandwidths (FWHM, full width and half maximum), and their intensities were selected based on results from previous studies of natural abundance and isotopically labeled deoxyHb[29] and oxyHb.[30] Regarding the general fitting strategy, the minimum bandwidths needed to fit a strong isolated band, such as the III/IV mode of the deoxy forms, was estimated to be 11 cm^{-1}. However, in trying to fit complex envelopes (e.g., between 400 and 450 cm^{-1}) it was decided to allow the widening of the fixed bandwidths to increase (by no more than 14 to 17 cm^{-1}) in an attempt to keep the number of included modes to the minimum. In fitting the spectra of deuterated analogues of a given protein, occasionally the bandwidth for those modes that exhibit relatively large shifts were increased by 1 or 2 cm^{-1} to improve fits. This is judged to be valid based on the knowledge that the percentage of deuteration is not 100%, although it is known to be between 90 and 95%; i.e., the incomplete deuteration can obviously cause some slight additional broadening.

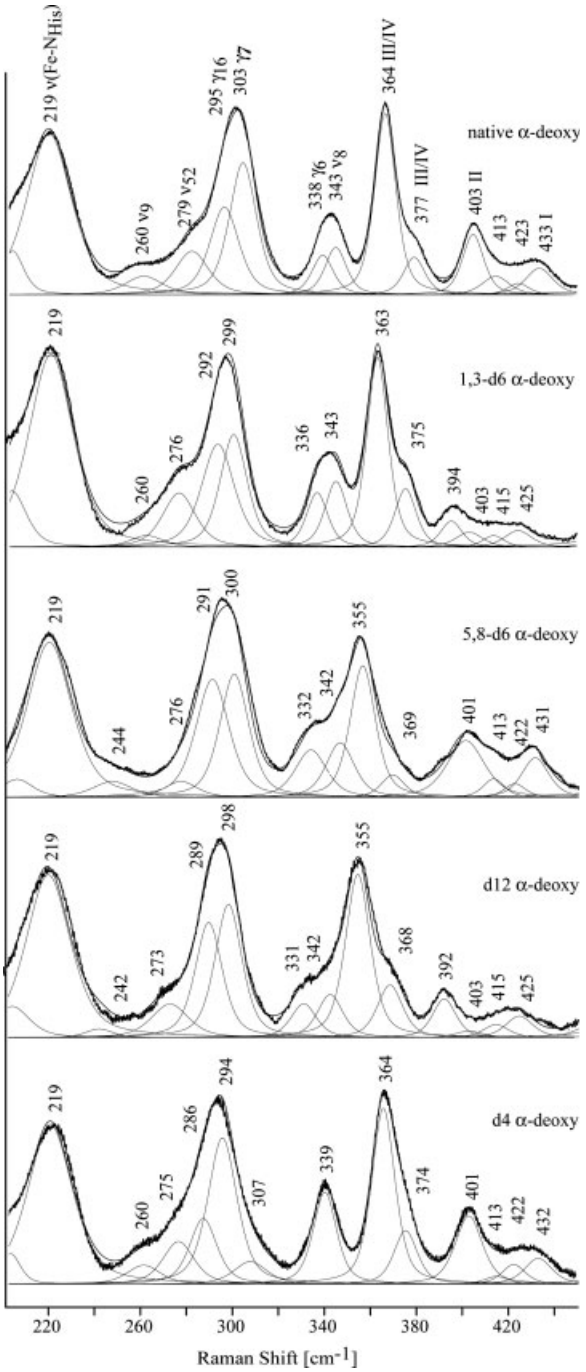

FIGURE 2 Deconvoluted resonance Raman spectra of α-deoxy subunit and its deuterated derivatives.

RESULTS AND DISCUSSION

Deoxy Forms

Figures 2 and 3 show the spectra of deoxy forms of the native and deuterated analogues of the α and β subunits. Within each set of spectral traces the spectra were normalized to the ν(Fe-N_{His}) bands at 219 cm^{-1} (α) or 223 cm^{-1} (β); these bands do not shift upon deuteration of the methine positions or the peripheral substituents. To provide better estimates of actual frequencies and reveal individual bands within complex overlapping spectral envelopes, deconvolution proce-

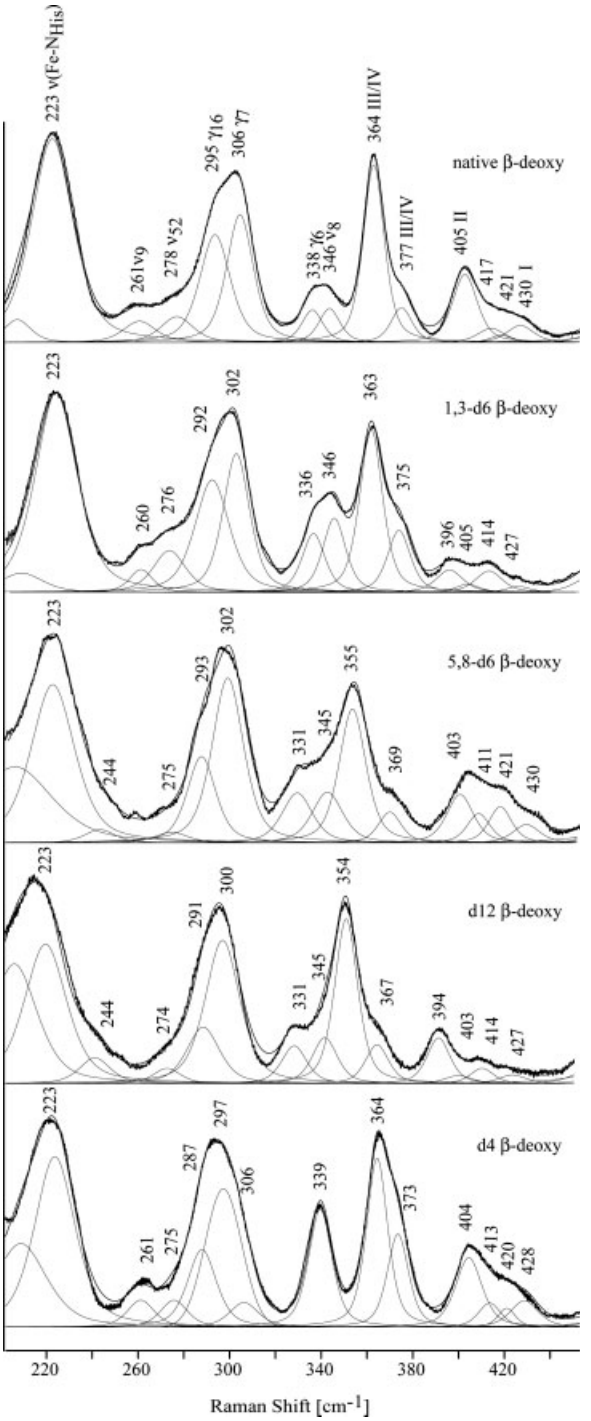

FIGURE 3 Deconvoluted resonance Raman spectra of β-deoxy subunit and its deuterated derivatives.

dures were applied as described under Experimental. The RR spectral data so derived are summarized for the deoxy forms in Table I.

Pyrrole I and II Deformation or So-Called "Vinyl Bending" Modes. The RR bands in the 400–440 cm^{-1} region are usually assigned to the "vinyl bending" vibrations, based on the fact that these modes have been shown to shift upon deuteration of one or both vinyl groups.[23,24,26,50] In the case of deoxyMb, as is seen for the deoxyHb subunit spectra given here, there are two dominant peaks, one being observed near 400 cm^{-1} and the other at higher frequency, near 435 cm^{-1}. In the case of myoglobin, selective labeling studies showed that the lower frequency mode is probably associated with the 4-vinyl group on pyrrole II, while the labeling of the 2-vinyl group on pyrrole I yields a smaller, but detectable shift of the higher frequency mode.[23,24,26,50] The spectra observed here, as well as those observed in an earlier study on methyl deuterated Mb derivatives,[31] clearly demonstrate that these features shift substantially upon deuteration of the 1 and 3 methyl groups (see the traces for the 1,3-*d*6-protoheme and *d*12-protoheme reconstituted analogues of the α and β subunits in Figures 2 and 3, where shifts of approximately 7–11 cm^{-1} are evident). Such shifts imply that these modes, nominally designated as vinyl bending modes,[23,24,26,28–35,51,52] actually contain significant contributions from macrocycle deformations involving the adjacent methyl groups; we note that experimental evidence for such complications was originally observed and reported by Hu et al.[26] in their study of Mb derivatives reconstituted with a so-called 6,7-diD$_2$ protoheme that actually contained (a total of 14) deuterium atoms situated at the C$_b$ (4), 1- and 3- methyls (6), and C$_d$ (4) positions shown in Figure 1. Moreover, as described below, these modes between 400–440 cm^{-1}, which apparently are more reasonably formulated as deformations involving the I or II pyrrole rings, are not shifted substantially upon deuteration of the 5 and 8 methyl groups; i.e., shifts of less than 3 cm^{-1} are observed for these two modes in the spectra of the 5,8-*d*6-protoheme and *d*12-protoheme reconstituted derivatives, data that support the designation to modes localized on pyrrole rings I and II. It is noted that there are a few unexpected *apparent* differences between isotopic shifts for the α and β subunits; e.g., the 433 cm^{-1} (α) and 430 cm^{-1} (β) lines of the deoxy samples listed in Table I exhibit different shifts for the 1,3-*d*6 and *d*12 analogues. Such apparent discrepancies are encountered in some cases in which one or both lines of the isotopomers are weak or overlapped with stronger features and thus should not be considered as confirmed differences.

Given the apparent propriety of formulating these modes as somewhat complex combinations of vinyl bending *and* pyrrole deformations, it seems important to reconsider their utility as direct probes of vinyl group disposition with respect to the pyrrole or aver-

Table I Summary of Deconvoluted Frequencies for Deoxy Forms of α and β Subunits and Their Deuterated Analogues

Mode	Assignment	Native α-Deoxy (Δ of 1,3-*d*6/5,8-*d*6/*d*12/*d*4)	Native β-Deoxy (Δ of 1,3-*d*6/5,8-*d*6/*d*12/*d*4)
ν(Fe-N_{His})		219 (0/0/0/0)	223 (0/0/0/0)
ν_9	$\delta(C_\beta C_l)_{sym}$	260 (0/16/18/0)	261 (1/17/17/0)
ν_{52}	$\delta(C_\beta C_l)_{sym}$	279 (3/3/6/4)	278 (2/3/4/3)
γ_{16}	Pyr. tilt	295 (3/4/6/9)	295 (3/2/4/8)
γ_7	$\gamma(C_\alpha C_m)$ + pyr. tilt	303 (4/3/5/9)	306 (4/4/6/9)
γ_6	Pyr. tilt	338 (2/6/7/31)	338 (2/7/7/32)
ν_8	ν (Fe-$N_{pyr.}$)	343 (0/1/1/4)	346 (0/1/1/7)
	$\delta(C_\beta C_c C_d)$ + pyr.	364 (1/9/9/0)	364 (1/9/10/0)
	$\delta(C_\beta C_c C_d)$ + pyr.	377 (2/8/9/3)	377 (2/8/10/4)
	$\delta(C_\beta C_a C_b)$ + pyr.	403 (9/2/11/2)	405 (9/2/11/1)
	$\delta(C_\beta C_a C_b)$ + pyr.	413 (10/0/10/0)	417 (12/6/14/4)
	$\delta(C_\beta C_a C_b)$ + pyr.	423 (8/1/8/1)	421 (7/0/7/1)
	$\delta(C_\beta C_a C_b)$ + pyr.	433 (8/2/8/1)	430 (3/0/3/2)

age plane of the heme macrocycle as has been suggested in various works.[28,34,35,52] Clearly, inasmuch as interactions of the methyl groups with active site residues are likely to be much less than those of the vinyl (or propionate groups, *vide infra*), it is reasonable to expect that the main determinant of the frequencies of such modes would be vinyl group (or propionate group) disposition. However, deducing the frequency dependence of these complex low frequency modes on such peripheral group orientations may not be as straightforward as is the case for more isolated modes. Thus, one of the most systematic attempts to document the effects of vinyl group disposition on the associated vinyl group frequencies is the recent comprehensive analysis reported by Marzocchi and Smulevich[53] of the ν(C=C) vibrations. These workers derive a straightforward quantitative relationship between the frequency of this stretching mode and the dihedral angle between the $C_\alpha C_\beta C_a$ and $C_\beta C_a C_b$ planes and provide convincing arguments for the reliability of this *relatively isolated* internal vinyl group mode and the specified structural parameter. However, given the as yet unspecified compositions of the low frequency "vinyl bending" (or propionate, *vide infra*) modes, caution seems warranted in trying to infer structural parameters from the observed frequencies. Thus, inspection of structures published for the set of closely related proteins being considered here, including deoxyMb[3] and the α and β subunits of hemoglobin,[4–6] an obvious correlation is not evident; i.e., measuring the vinyl group orientations with respect to the pyrrole average plane (or as measured by the definition used by Marzocchi and Smulevich[53]) reveals significantly different vinyl group orientations for Mb (34 and 5°) compared with the subunits (e.g., for α deoxy the two angles are 54 and 47°), but quite similar RR spectra are observed in the 400–450 cm^{-1} range. It is pointed out that Marzocchi and Smulevich[53] also did not attempt to correlate vinyl group disposition with these low frequency modes. In fact, in an earlier study of the low frequency modes of cytochrome *c* peroxidase, Smulevich and coworkers[52] noted changes in behavior of these modes upon changes in pH and specifically pointed out that such behavior could arise by several different mechanisms or combinations thereof. Thus, while there have been previous attempts to relate the frequencies of these modes to vinyl group orientation, further careful inspection of more comprehensive data sets will be required to evaluate the utility of these modes for specifying structural changes.

Pyrrole III and IV Deformations or So-Called "Propionate Bending" Modes. Modes appearing between $\sim$ 360 and 380 cm^{-1} in the RR spectra of heme proteins, often some of the strongest features in the low frequency region, are traditionally associated with "propionate bending" motions.[15,16,25–35,52] However, as pointed out in a recent RR study of deoxy and ligated myoglobins[31] and cytochrome $P450_{camphor}$,[33] these modes also exhibit substantial shifts to lower frequency (by up to 15 cm^{-1}) upon deuteration of the 5 and 8 methyl groups, suggesting a proper formulation as "pyrrole III and IV" deformations. Similar behavior is observed here for the subunits of hemoglobin A as shown in Figures 4 and 5. Thus, the bands

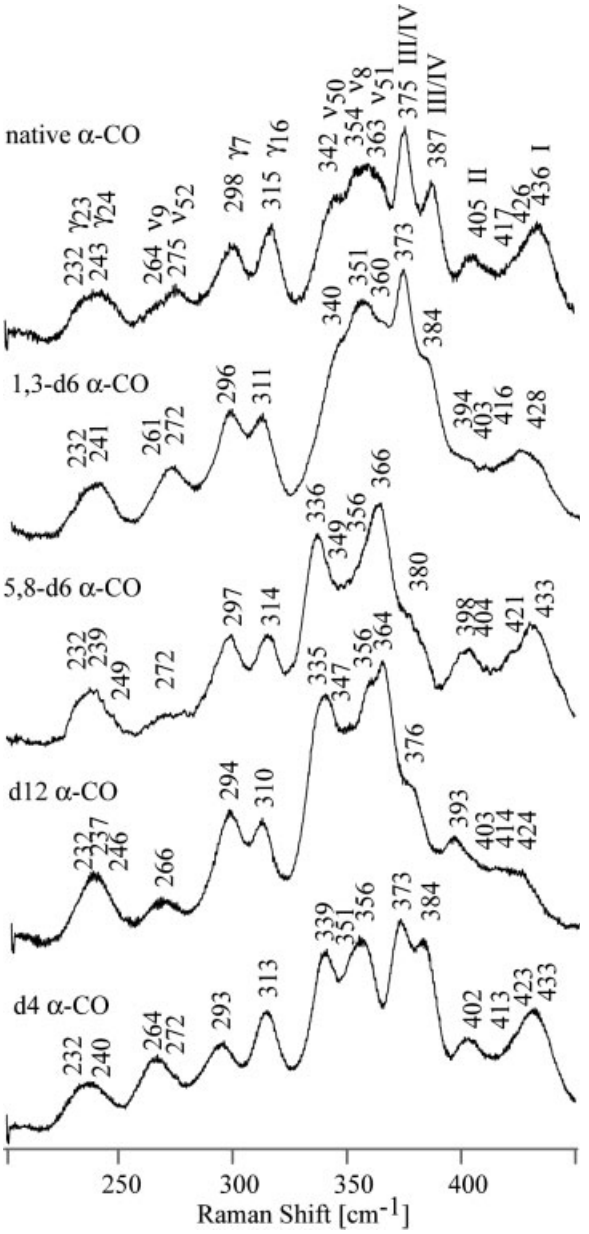

FIGURE 4 Resonance Raman spectra of α-CO subunit and its deuterated derivatives.

at 364 and 377 cm^{-1} in the spectra of both the α and β subunits shift for the 5,8-*d*6-protoheme–containing protein by 8–10 cm^{-1} and by 10–11 cm^{-1} in the spectra of the *d*12-protoheme reconstituted samples. Consistent with the observations made for the I and II pyrrole deformations described above, these modes exhibit quite small shifts (1–2 cm^{-1}) in the spectra of the 1,3–6-protoheme reconstituted proteins, indicating that these peripheral group sensitive modes are at least segregated on different sides of the macrocycle. The question of whether a given mode might correspond to a more restricted fragment of the macrocycle (i.e., the pyrrole III, 6-propionate, or pyrrole IV, 7-propionate) cannot be unambiguously established without further work employing hemes bearing specifically labeled propionate groups.

Again, while the frequencies of these modes have sometimes been suggested to report on the disposition of the propionates with respect to orientation or hydrogen bonding to active site residues or water,[27,28,34,35] the reliability of such structural inferences is not firmly established; although Friedman and coworkers,[28] as well as Schelvis and co-

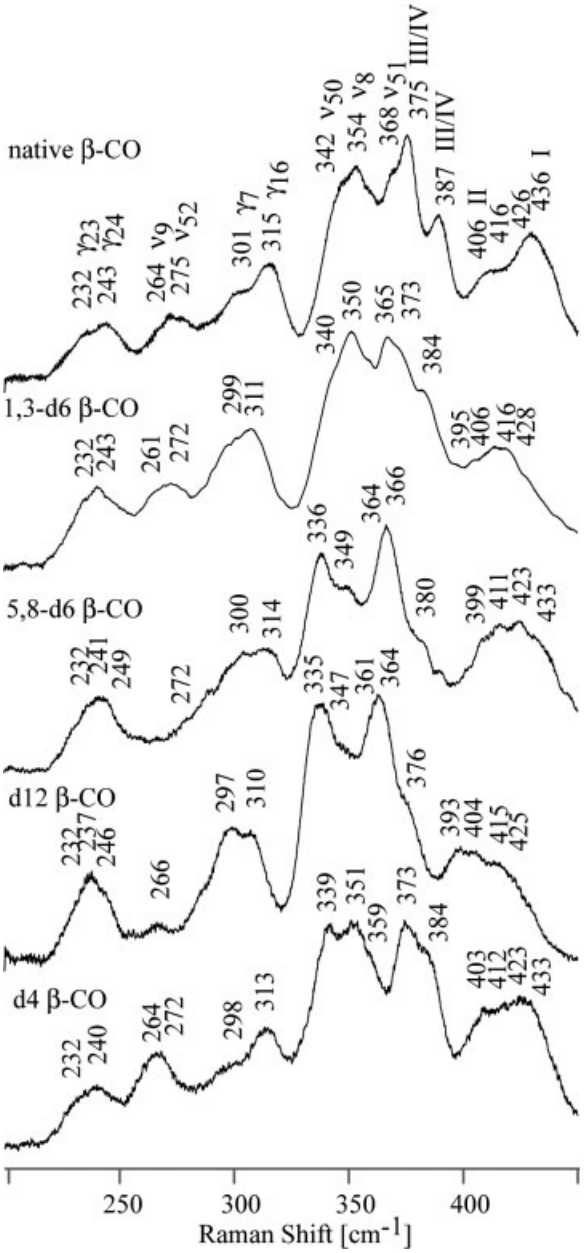

FIGURE 5 Resonance Raman spectra of β-CO subunit and its deuterated derivatives.

workers,[34,35] have provided logical arguments to support such suggestions, further definition of such relationships will require the availability and study of a large group of proteins bearing new specifically labeled hemes and a thorough analysis of a correspondingly comprehensive set of structural data.

Heme Macrocycle Modes. In addition to the modes that have been traditionally associated with the vinyl and propionate peripheral groups, there are a number of in-plane and out-of-plane heme deformation modes in this low frequency region that may serve to report on macrocycle out-of-plane distortions.[20,25,26,29,36,37] As first pointed out by Friedman and coworkers,[28] the overlapped υ_8 and γ_6 modes appearing near 340 cm^{-1} are not well separated when the pyrrole III/IV mode occurs below 370 cm^{-1} as is the case for both of the Hb subunits being studied here. In the case of deoxy Mb, where this III/IV mode occurs at 370 cm^{-1}, the ν_8 and γ_6 modes are better resolved as separate features occurring at 342 and 332 cm^{-1}, respectively.[28,31] In the spectra of the β subunit (Figure 5) there is distinct evidence for two bands in this region, whereas in the case of the α subunit (Figure 4), the two bands are apparently too closely overlapped to be distinguished. However, as in the case of the labeled Mb derivatives studied earlier,[31] they are more easily distinguished in the spectra of the 5,8-*d*6-protoheme reconstituted subunits, because the lower frequency component experiences a shift to lower frequency while the higher frequency component is relatively insensitive.

In reality, it becomes difficult to make definitive assignments of these modes in the absence of supportive normal mode calculations. Thus, the lower frequency component here is being assigned to the γ_6 mode in compliance with the assignment originally suggested by Hu et al.[26] for met-Mb, and is being correlated with the very weak "extra intensity" located near 307 cm^{-1} in the spectrum of the *d*4-protoheme analogue; this feature is included in the fitting procedure for the *d*4-analogue, but actually there is not strong evidence for including it. Clearly, it is also reasonable to suggest that the two overlapped features observed between 330 and 350 cm^{-1} have different isotope sensitivities than those suggested here and previously,[26,31] with the lower frequency mode being insensitive to *d*4-substitution and directly overlapped with the higher frequency mode that shifts down by about 4–5 cm^{-1} in the methine-deuterated samples.

One of the most interesting features in the low frequency RR spectra of heme proteins is the γ_7 mode, which occurs near 300 cm^{-1} and is unusually strong in the spectra of the deoxy forms of both hemoglobin

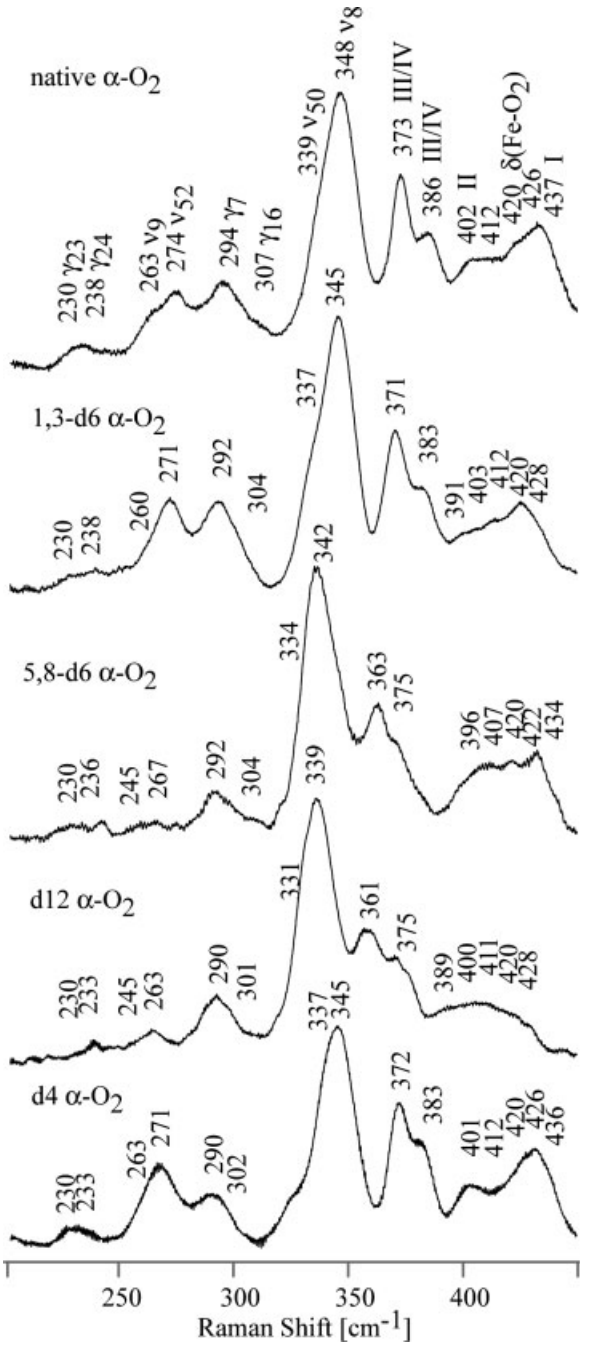

FIGURE 6 Resonance Raman spectra of α-O_2 subunit and its deuterated derivatives.

subunits. This mode is activated by the strong distortion of the heme in the deoxy forms (compared with the more planar geometry of the met- and ligated forms in Figures 4–7, or even the deoxy form of Mb[31]). Its precise frequency and the magnitude of shifts observed for the various deuterated analogues are uncertain owing to overlap with other modes in this region, giving rise to an envelope of features

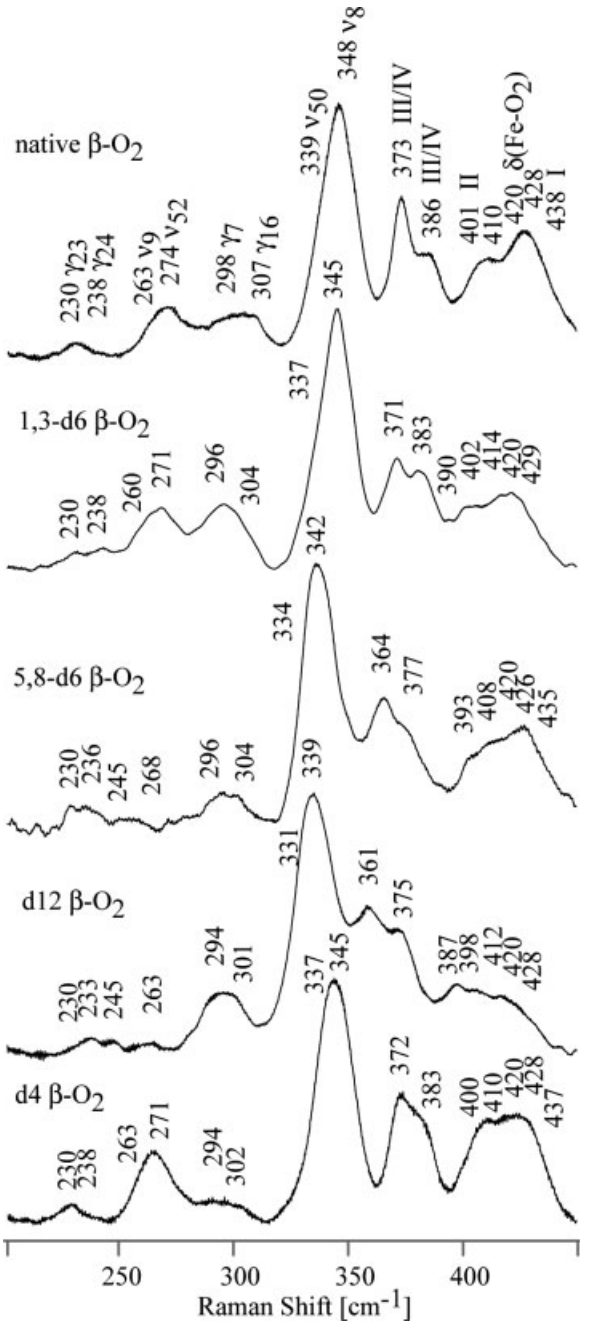

FIGURE 7 Resonance Raman spectra of β-O_2 subunit and its deuterated derivatives.

between about 260 and 300 cm^{-1}. Thus, the broad intense band centered near 300 cm^{-1} is apparently composed of two relatively strong features that appear to occur at 303 and 295 cm^{-1} for the α subunits and 306 and 295 cm^{-1} in the case of the β subunits, the bands being better resolved in the latter case (Figure 3). According to the well-documented mode formulations derived for model systems,[17,20–22] the γ_7 mode involves out-of-plane distortions of the methine carbons and pyrrole units and therefore would be expected to exhibit significant shifts for the *d*4-protoheme–substituted and methyl–deuterated proteins, as is the case for the higher frequency component, shifting by about 6–9 cm^{-1} for the *d*4- and *d*12- analogues (as derived by the deconvolution procedure being used here). Similar behavior is observed for the lower frequency component tentatively being assigned to another low frequency out-of-plane mode expected in this region, γ_{16}. Comparison with assignments from earlier works on metalloporphyrins and heme proteins[17–22,25,26] prompts the tentative assignments given in the Figures 2 and 3 and Table I; i.e., the 295 cm^{-1} component is assigned to γ_{16} and the 279 cm^{-1} to ν_{52}. However, it is important to note that other interpretations of this envelope are possible. Thus, the reason for including two strong components at about 295 and 303 cm^{-1} in the deconvolution procedure for the α subunits, rather than one broader single band, is that there are clearly two strong bands at these positions in the spectra of the β subunits, as evidenced by the noticeable double maximum. However, it is noted that the β subunits form a β_4 tetramer in solution and this tetramer has been shown by X-ray crystallography to possess hemes with differing degrees of planarity[6]; i.e., it seems possible that the two features observed near 300 cm^{-1} in the spectra of the β subunits are ascribable to two γ_7 modes, while the α subunits might exhibit a single, though broadened, γ_7 mode.

Finally, some comments are required for the weak feature observed near 260 cm^{-1}, which is being assigned to ν_9. This assignment is somewhat problematic, because the frequency seems to be rather high compared with the relatively strong mode observed at 240 cm^{-1} that has been previously assigned to ν_9 for deoxy Mb and its mutants.[28] Alternatively, it could be reasonably ascribed to γ_{23}, which is expected in this frequency region and is also normally rather insensitive to methine deuteration.[17–22] Such an assignment would imply the ν_9 mode is not observed in these hemoglobin derivatives, a suggestion that would conform to the behavior noted by Friedman and coworkers[28] in a series of Mb mutants, wherein it was shown that whenever the "propionate bending" mode (designated III/IV pyrrole deformation here) occurs near 370 cm^{-1} the ν_9 is clearly observable, but when the III/IV deformation falls to about 365 cm^{-1}, the ν_9 is weakened or buried within the strong, broad ν(Fe-N_{his}).

Ligated Forms

Figures 4 and 5 show the spectra of CO adducts of the natural abundance and deuterated analogues of the α and β subunits, respectively, while the spectra

Table II Summary of Deconvoluted Frequencies for CO Adducts of α and β Subunits and Their Deuterated Analogues

Mode	Assignment	Native α-CO (Δ of 1,3-*d*6/5, 8-*d*6/*d*12/*d*4)	Native β-CO (Δ of 1,3-*d*6/5, 8-*d*6/*d*12/*d*4)
γ_{23}	Pyr. tilt	232 (0/0/0/0)	232 (0/0/0/0)
γ_{24}	$\gamma(C_\alpha C_m)$	243 (2/4/6/3)	243 (0/2/6/3)
ν_9	$\delta(C_\beta C_l)_{sym}$	264 (3/15/18/0)	264 (3/15/18/0)
ν_{52}	$\delta(C_\beta C_l)_{sym}$	275 (3/3/9/3)	275 (3/3/9/3)
γ_7	$\gamma(C_\alpha C_m)$ + pyr. tilt	298 (2/1/4/5)	301 (2/1/4/3)
γ_{16}	Pyr. tilt	315 (4/1/5/2)	315 (4/1/5/2)
ν_{50}	$\nu(MN_{pyr}) + \gamma(C_\beta C_l) + \delta(C_\beta C_l)$	342 (2/6/7/3)	342 (2/6/7/3)
ν_8	$\nu(MN_{pyr}) + \gamma(C_\beta C_l) + \delta(C_\beta C_l)$	354 (3/5/7/3)	354 (4/5/7/3)
ν_{51}	$\delta(C_\beta C_l)_{asym}$	363 (3/7/7/7)	368 (3/4/7/9)
	$\delta(C_\beta C_c C_d)$ + pyr.	375 (2/9/11/2)	375 (2/9/11/2)
	$\delta(C_\beta C_c C_d)$ + pyr.	387 (3/7/11/3)	387 (3/7/11/3)
	$\delta(C_\beta C_a C_b)$ + pyr.	405 (11/7/12/3)	406 (11/7/13/3)
	$\delta(C_\beta C_a C_b)$ + pyr.	417 (14/13/14/4)	416 (10/5/12/4)
	$\delta(C_\beta C_a C_b)$ + pyr.	426 (10/5/12/3)	426 (10/3/11/3)
	$\delta(C_\beta C_a C_b)$ + pyr.	436 (8/3/12/3)	436 (8/3/11/3)

of the corresponding O_2 adducts are given in Figures 6 and 7. The frequencies and deuterium shifts are summarized in Tables II and III. While not shown in the spectra presented herein, the ν(Fe-CO) stretching and δ(Fe-C–O) bending modes are observed in the spectra of both the α and β subunits at 505 and 577 cm^{-1}, respectively. Also, the $\nu(Fe\text{-}O_2)$ mode is observed at 570 cm^{-1} in the spectra of both oxygenated subunits.

The spectra of the ligated forms contain many of the same modes identified for the deoxy forms and exhibit comparable shifts, but several general observations are of interest. Obviously, the strong $\nu(Fe\text{-}N_{His})$ mode is missing in the spectra of the ligated form, but two new out-of-plane modes, γ_{23} and γ_{24}, appear as weak features near 230 and 240 cm^{-1}. Owing to the higher degree of planarity of the heme macrocycle in the ligated forms, the γ_7 modes near 300 cm^{-1} are correspondingly weak. The region near ν_8 between about 330 and 360 cm^{-1} is quite congested, with contributions of several in-plane and out-of-plane modes as delineated in

Table III Summary of Deconvoluted Frequencies for oxy Adducts of α and β Subunits and Their Deuterated Analogues

Mode	Assignment	Native α-O_2 (Δ of 1,3-*d*6/5, 8-*d*6/*d*12/*d*4)	Native β-O_2 (Δ of 1,3-*d*6/5, 8-*d*6/*d*12/*d*4)
γ_{23}	Pyr. tilt	230 (0/0/0/0)	230 (0/0/0/0)
γ_{24}	$\gamma(C_\alpha C_m)$	238 (0/2/5/5)	238 (0/2/5/5)
ν_9	$\delta(C_\beta C_l)_{sym}$	263 (3/18/18/0)	263 (3/18/18/0)
ν_{52}	$\delta(C_\beta C_l)_{sym}$	274 (3/7/11/3)	274 (3/6/11/3)
γ_7	$\gamma(C_\alpha C_m)$ + pyr. tilt	294 (2/2/4/4)	298 (2/2/4/4)
γ_{16}	Pyr. tilt	307 (3/3/6/5)	307 (3/3/6/5)
ν_{50}	$\nu(MN_{pyr}) + \gamma(C_\beta C_l) + \delta(C_\beta C_l)$	339 (2/5/8/2)	339 (2/5/8/2)
ν_8	$\nu(MN_{pyr}) + \gamma(C_\beta C_l) + \delta(C_\beta C_l)$	348 (3/6/9/3)	348 (3/6/9/3)
	$\delta(C_\beta C_c C_d)$ + pyr.	373 (2/10/12/1)	373 (2/9/12/1)
	$\delta(C_\beta C_c C_d)$ + pyr.	386 (3/11/11/3)	386 (3/9/11/3)
	$\delta(C_\beta C_a C_b)$ + pyr.	402 (11/6/13/1)	401 (11/8/14/1)
	$\delta(C_\beta C_a C_b)$ + pyr.	412 (9/5/12/0)	410 (8/2/12/0)
	$\delta(Fe\text{-}O_2)$	420 (0/0/0/0)	420 (0/0/0/0)
	$\delta(C_\beta C_a C_b)$ + pyr.	426 (14/4/15/0)	428 (14/2/16/0)
	$\delta(C_\beta C_a C_b)$ + pyr.	437 (9/3/9/1)	438 (9/3/10/1)

Tables II and III. Finally, it is noted that the higher ($\sim$ 387 cm^{-1}) of the two modes designated as pyrrole III/IV deformations, involving propionate motions, is now noticeably more intense relative to the lower frequency mode, perhaps suggesting altered interactions with the active site environment.[27,28,33–35] Similarly, for the ligated subunits, the higher ($\sim$ 435 cm^{-1}) of the two I/II pyrrole deformations, involving vinyl group bending, is more intense than the lower frequency mode observed near 405 cm^{-1}, in contrast to the deoxy forms. As mentioned above, the structural significance of such differences will require further work for clarification.

CONCLUSION

The availability of selectively deuterated protoheme analogues helps establish the involvement of various molecular fragments of the heme, in particular vibrational modes, and these data are needed to elucidate the nature of these structure-sensitive low frequency modes. However, the rather large shifts observed for given modes upon deuteration of different fragments (e.g., large and comparable shifts observed for I/II pyrrole deformations upon methyl *or* vinyl group deuteration) reveal the need to apply systematic theoretical studies to unravel the nature of these modes to gain a practically reliable interpretational framework. On the other hand, the relatively large frequency shifts inducible by methyl group deuteration do provide a relatively convenient strategy for editing spectral changes in complex, multicomponent systems, giving rise to distinct signals arising from the highly deuterated hemes in these multiheme systems. Resonance Raman and time-resolved RR studies of chemically intact hemoglobin tetramers, bearing deuterated hemes in only one type of subunit (i.e., α or β subunits),[12] have already demonstrated this utility and studies employing similar strategies are continuing.[54]

This work was supported by a grant (DK35153 to J.R.K.) from the National Institutes of Health. Partial support from the Pfletschinger Habermann Fund of Marquette University is also acknowledged by J.R.K. Dr. Edyta Podstawka was a Fellow of Jagiellonian University Rector Foundation.

REFERENCES

1. Antonini, E.; Rossi-Bernardi L.; Chiancone, E., Eds.; In Methods in Enzymology; Academic Press: New York, 1981; Vol. 76.
2. Fermi, G.; Perutz, M. F.; Sanan, B.; Fourme, R. J Mol Biol 1984, 175, 159–174.
3. Vojtechovsky, J.; Chu, K.; Berendzen, J.; Sweet, R. M.; Schlichting, I. Biophys J 1999, 77, 2153–2174.
4. Yang, F.; Phillips, G. N. J Mol Biol 1996, 256, 762–774.
5. Shaanan, B. J Mol Biol 1983, 171, 31–59.
6. Borgstahl, G. E. O.; Rogers, P. H.; Arnone, A. J Mol Biol 1994, 236, 831–843.
7. Rousseau, D. L.; Friedman, J. M. In Biological Applications of Raman Spectroscopy; Spiro, T. G., Ed.; Wiley & Sons: New York, 1988; Vol. 3, pp. 133–215.
8. Friedman, J. M. In Methods in Enzymology; Everse, J., Vandegriff, K. D., Winslow, R. M., Eds.; Academic Press: San Diego, 1994; Vol. 232, pp. 205–231.
9. Dasgupta, S.; Spiro, T. G. Biochemistry 1986, 25, 5941–5948.
10. Jayaraman, V.; Rodgers, K. R.; Mukerji, I.; Spiro, T. G. Science 1995, 269, 1843–1848.
11. Kitagawa, T. In Biological Applications of Raman Spectroscopy; Spiro, T. G., Ed.; Wiley & Sons: New York, 1988, Vol. 3, pp. 97–131.
12. Kincaid, J. R.; Rajani, C.; Proniewicz, L. M.; Maruszewski, K. J Am Chem Soc 1997, 119, 9073–9074.
13. Woodruff, W. H.; Farquharson, S. Science 1978, 201, 831–833.
14. Findsen, E. W.; Friedman, J. M.; Ondrias, M. R.; Simon, S. R. Science 1985, 229, 661–665.
15. Spiro, T. G. Adv Protein Chem 1985, 37, 111–159.
16. Kincaid, J. R. In The Porphyrin Handbook; Kadish, K. M.; Smith, K. M.; Guilard, R., Eds. Academic Press: San Diego, 2000; Vol 7, pp. 225–291.
17. Kitagawa, T.; Abe, M.; Ogoshi, H. J. Chem Phys 1978, 69, 4516–4525.
18. Abe, M.; Kitagawa, T.; Kyogoku, Y. Chem Phys 1978, 69, 4526.
19. Li, X.-Y.; Czernuszewicz, R. S.; Kincaid, J. R.; Stein, P. B.; Spiro, T. G. J Phys Chem 1990, 94, 47–61.
20. Li, X.-Y.; Czernuszewicz, R. S.; Kincaid, J. R.; Spiro, T. G. J Am Chem Soc 1989, 111, 7012–7023.
21. Hu, S.; Mukherjee, A.; Piffat, C.; Mak, R. S. W.; Li, X.-Y.; Spiro, T. G. Biospectroscopy 1995, 1, 396–412.
22. Stoll, L. K.; Zigierski, M. Z.; Kozlowski, P. M. J Phys Chem A 2002, 106, 170–175.
23. Choi, S.; Spiro, T. G. J Am Chem Soc 1982, 104, 4337–4344.
24. Choi, S.; Spiro, T. G.; Langry, K. C.; Smith, K. M.; Budd, D. L.; La Mar, G. N. J Am Chem Soc 1982, 104, 4345–4351.
25. Hu, S.; Morris, I. K.; Singh, J. P.; Smith, K. M.; Spiro, T. G. J Am Chem Soc 1993, 115, 12446–12458.
26. Hu, S.; Smith, K. M.; Spiro, T. G. J Am Chem Soc 1996, 118, 12638–12646.
27. Cerda-Colon, J. F.; Silfa, E.; Lopez-Garriga, J. J Am Chem Soc 1998, 120, 9312–9317.
28. Peterson, E. S.; Friedman, J. M.; Chien, E. Y. T.; Sligar, S. G. Biochemistry 1998, 37, 12301–12319.
29. Podstawka, E.; Rajani, C.; Kincaid, J. R.; Proniewicz, L. M. Biopolymers (Biospectroscopy) 2000, 57, 201–207.
30. Podstawka, E.; Kincaid, J. R.; Proniewicz, L. M. J Mol Struct 2001, 596, 157–162.

31. Mak, P. J.; Podstawka, E.; Kincaid, J. R.; Proniewicz, L. P. Biopolymers 2004, 75, 217–228.
32. Nagai, M.; Aki, M.; Li, R.; Jin, Y.; Sakai, H.; Nagatomo, S.; Kitagawa, T. Biochemistry 2000, 39, 13093–13105.
33. Manyumwa, M. E.; M.S. Thesis, Marquette University, 2005.
34. Chen, Z.; Ost, T. W. B.; Schelvis, J. P. M. Biochemistry 2004, 43, 1798–1808.
35. Chen, Z.; Wang, L. H.; Schelvis, J. P. M. Biochemistry 2003, 42, 2542–2551.
36. Shelnutt, J. A. In The Porphyrin Handbook; Kadish, K. M.; Smith, K. M.; Guilard, R., Eds.; Academic Press: San Diego, 2000; Vol. 7, pp. 167–224.
37. Zbylut, S. D.; Kincaid, J. R. J Am Chem Soc 2002, 124, 6751–6758.
38. DiNello, R. K.; Chang, C. K. In The Porphyrins: Structure and Synthesis; Dolphin D., Ed.; Academic Press: New York, 1978; Vol. 1 (Part A), pp. 289–294.
39. Fuhrhop, J.-H.; Smith, K. M. In Laboratory Methods: Porphyrin and Metalloporphyrins; Smith, K. M., Ed.; Elsevier/North Holland: Amsterdam, 1975; pp. 757–869.
40. Janson, T. R.; Katz, J. J. The Porphyrins: Physical Chemistry; Dolphin, D., Ed.; Academic Press, New York, 1979; Vol. 4 (Part B), pp. 1–59.
41. Kenner, G. W.; Smith, K. M.; Sutton, M. J Tetrahedron Lett 1973, 16, 1303–1306.
42. Godziela, G. M.; Kraner, S. K.; Goff, H. M. Inorg Chem 1986, 25, 4286–4288.
43. Barbush, M.; Dixon, D. W. Biochem Biophys Res Commun 1985, 129, 70–75.
44. Buchler, J. W. In The Porphyrins: Structure and Synthesis; Dolphin, D., Ed.; Academic Press: New York, 1978; Vol. 1 (Part A), pp. 389–483.
45. DiNello, R. K.; Dolphin, D. H. Anal Biochem 1975, 64, 444–449.
46. Riggs, A. In Methods in Enzymology; Antonini, E., Rossi-Bernardi, L., Chiancone, E., Eds.; Academic Press: New York, 1981; Vol. 76, pp. 5–29.
47. Yip, Y. K.; Waks, M.; Beychok, S. J Biol Chem 1972, 247, 7237–7244.
48. Smith, K. M.; Parish, D. W.; Inouye, W. S. J Org Chem 1986, 51, 666–671.
49. Jayarajah, S.; Kincaid, J. R. Biochemistry 1990, 29, 5087–5094.
50. Uchida, K.; Susai, Y.; Hirotani, E.; Kimura, T.; Yoneya, T.; Takeuchi, H.; Harada, I. J Biochem 1988, 103, 979–985.
51. Kalsbeck, W. A.; Ghosh, A.; Pandey, R. K.; Smith, K. M.; Bocian, D. F. J Am Chem Soc 1995, 117, 10959–10968.
52. Smulevich, G.; Hu, S.; Rodgers, K. R.; Goodin, D. B.; Smith, K. M.; Spiro, T. G. Biospectroscopy 1996, 2, 365–376.
53. Marzocchi, M. P.; Smulevich, G. J Raman Spectrosc 2003, 34, 725–736.
54. Zhao, X.; Balakrishnan, G.; Podstawka, E.; Proniewicz, L. M.; Kincaid, J. R.; Spiro, T. G. to be submitted for publication.

Reviewing Editor: Laurence Nafie